THE JOURNAL OF PHYSICAL CHEMISTRY B

Article

pubs.acs.org/JPCB

Modeling the [NTf_2] Pyridinium Ionic Liquids Family and Their Mixtures with the Soft Statistical Associating Fluid Theory Equation of State

M. B. Oliveira,[†] F. Llovell,[‡] J. A. P. Coutinho,[†] and L. F. Vega*[,‡,§]

[†]CICECO, Chemistry Department, University of Aveiro, Campus de Santiago, 3810-193 Aveiro, Portugal

[‡]MATGAS Research Center, Campus de la UAB, 08193 Bellaterra, Barcelona, Spain

[§]Carburos Metálicos/Air Products Group, C/Aragón 300, 08069 Barcelona, Spain

ABSTRACT: In this work, the soft statistical associating fluid theory (soft-SAFT) equation of state (EoS) has been used to provide an accurate thermodynamic characterization of the pyridinium-based family of ionic liquids (ILs) with the bis(trifluoromethylsulfonyl)imide anion [NTf_2]$^-$. On the basis of recent molecular simulation studies for this family, a simple molecular model was proposed within the soft-SAFT EoS framework. The chain length value was transferred from the equivalent imidazolium-based ILs family, while the dispersive energy and the molecular parameters describing the cation−anion interactions were set to constant values for all of the compounds. With these assumptions, an appropriate set of molecular parameters was found for each compound fitting to experimental temperature−density data at atmospheric pressure. Correlations for the nonconstant parameters (describing the volume of the IL) with the molecular weight were established, allowing the prediction of the parameters for other pyridiniums not included in the fitting. Then, the suitability of the proposed model and its optimized parameters were tested by predicting high-pressure densities and second-order thermodynamic derivative properties such as isothermal compressibilities of selected [NTf_2] pyridinium ILs, in a large range of thermodynamic conditions. The surface tension was also provided using the density gradient theory coupled to the soft-SAFT equation.

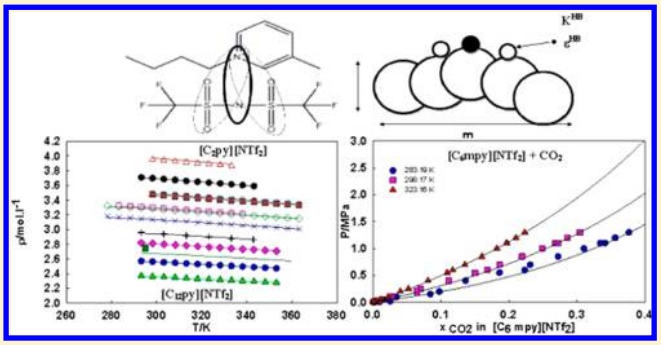

Finally, the soft-SAFT EoS was applied to describe the phase behavior of several binary mixtures of [NTf_2] pyridinium ILs with carbon dioxide, sulfur dioxide, and water. In all cases, a temperature-independent binary parameter was enough to reach quantitative agreement with the experimental data. The description of the solubility of CO_2 in these ILs also allowed identification of a relation between the binary parameter and the molecular weight of the ionic liquid, allowing the prediction of the CO_2 + C_{12}py[NTf_2] mixture. The good agreement with the experimental data shows the excellent ability of the soft-SAFT EoS to describe the thermophysical properties of ILs as well as their phase behavior. Results prove that this equation of state can be a valuable tool to assist the design of ILs (in what concerns cation and anion selection) in order to obtain ILs with the desired properties and, consequently, enhancing their potential industrial applications.

1. INTRODUCTION

During the past decade, ionic liquids (ILs) have drawn academic and commercial attention due to their unusual chemical and physical properties that make them valuable alternatives to traditional compounds for different applications, such as separation and extraction processes. A considerable volume of research and review works have been published addressing their valuable properties and how they can be designed for a specific application by matching different anions and cations.[1,2]

Most of the experimental and modeling work in ILs addresses those with an imidazolium as a cation.[3] Their easy synthesis can explain that preference, but there are other families of ILs of interest, although much less studied, such as the pyridinium cation based, addressed on this work. Compared to the imidazolium cations, the pyridiniums have a lower cost. In addition, they are less toxic and chemically more stable and have a high extractive performance.[4−6] In fact, some research works concerning their possible applications have already been reported, showing, for instance, how effective they can be for the selective removal of aromatic heterocyclic sulfur compounds from diesel at room temperature,[6] and how they can be applied to enhance speed and product yield of organic reactions such as the Diels−Alder.[7]

As mentioned above, little research has been focused on pyridinium ILs. The review presented by Coutinho et al.[8]

Received: April 3, 2012
Revised: May 28, 2012
Published: June 19, 2012

dx.doi.org/10.1021/jp303166f | J. Phys. Chem. B 2012, 116, 9089−9100

summarizes a group of predictive methods developed up to now to estimate IL thermophysical properties. Most of the works published to date are empirical methods applied on the modeling of the thermodynamic and transport properties of pyridinium-based pure ILs. Coutinho and co-workers applied the Tait equation[9] and also an extension of the Ye and Shreeve's group contribution method[10] to correlate density−temperature and density−pressure dependencies for several pyridinum-based ILs, while Paduszyński and Domańska[11] proposed a group contribution method for the same purpose. Mokhtarani et al.[12] and Sánchez et al.[13] proposed a linear fit to correlate the temperature dependency of densities of pure pyridinium-based ILs and their binary mixtures with water, while they applied the Vogel−Fulcher−Tammann (VFT) equation for viscosity calculations. Bandrés et al.[14] and Dutt and Ravikumar[15] proposed correlations based on the Hole theory and on the reduced form of the Arrhenius model, respectively, for surface tensions. Gardas and Coutinho[16] proposed a group contribution method for pyridinium-based-IL isothermal compressibilities and isobaric expansivities. Quantitative structure−activity relationship (QSAR) models were applied for the estimation of the melting points of those ILs.[8] Very recently, a new paper from Paduszyński and Domańska[17] has used a molecular-based equation of state (PC-SAFT) to model several thermophysical properties of several families of ILs with the $[Tf_2N]$ anion and different cations, including the pyridiniums. They modeled the ionic liquids using 10 associating sites to represent the cation−anion interactions. The work is very extensive and physically well-grounded, including the calculation of the temperature−density diagram, the two-phase equilibrium, the vapor pressure, the enthalpy of vaporization, and the surface tension of several compounds.

Several efforts have been made toward the description of the phase behavior of pyridinium-based-IL mixtures, including activity coefficient models, equations of state, and quantum chemistry calculations. Among the activity coefficient models, the non-random two liquid (NRTL) model has been the most frequently applied: Dreiseitlová et al.[18] used that approach to describe the mutual solubilities of several pyridinium-based tetrafluoroborates ($[BF_4]^-$) and toluene; Crosthwaite et al.[19] correlated the phase equilibria of 1-*n*-butyl-3-methylpyridinium bis(trifluoromethylsulfonyl)imide ($[NTf_2]^-$) and the 1-*n*-hexylpyridinium $[NTf_2]$ binary mixtures with 1-butanol and 1-hexanol; Chapeaux et al.[20] computed the 1-octanol/water partition coefficients of eight pyridiniums; García et al.[21] correlated the liquid−liquid equilibria of four ternary systems containing heptane and toluene; and, finally, Domańska et al.[22] described the solid−liquid equilibria (SLE) and the liquid−liquid equilibria (LLE) of binary systems containing 1-butyl-4-methylpyridinium $[NTf_2]$ with water, alcohols, and alkanes. In addition, Lazzús and Marín[23] applied the NRTL, UNIQUAC, and Wilson models to correlate the vapor−liquid-equilibria (VLE) of 1-butyl-4-methylpyridinium tosylate $[TsO]^-$ binary systems with ethanol, 1-propanol, and 1-butanol. All models performed reasonably well, and none stands out in the description of these systems. The main drawback of activity coefficient models is the need of adjusting an important amount of parameters, many times temperature-dependent, to experimental data.

There are also several contributions done with equations of state to model those compounds. The hard-sphere equation of state (EoS) was applied to describe *PVT* properties of the 3-methyl-1-propylpyridinium with the $[NTf_2]^-$ anion,[24] apart from other ILs with other cations. The group contribution equation of state was used by Martín et al.[25] to correlate the VLE of CO_2, O_2, and SO_2 binary mixtures with 1-alkyl-3-methylpyridinium $[NTf_2]$ and 1-alkyl-1-methylpyrrolidinium $[NTf_2]$ ILs. This approach was then extended by Bermejo et al.[26] for ILs containing the same pyridinium cations but other anions different than the $[NTf_2]^-$. Moreover, the previously mentioned work of Paduszyński and Domańska[17] with PC-SAFT also includes the calculation of the LLE and SLE of different pyridininium ILs (among others) with *n*-alkylbenzenes and water. Binary corrections were adjusted to infinite dilution activity coefficients of a particular solute in a given IL determined experimentally or predicted by means of the modified UNIFAC (Dortmund) group contribution method.

Another approach usually adopted to describe the phase equilibria of ILs is the predictive method based on unimolecular quantum chemistry calculations, the conductor-like screening model for realistic solvation (COSMO-RS). Freire and co-workers used the COSMO-RS to qualitatively predict the LLE of the water + 3-methyl-1-propylpyridinium $[NTf_2]$ system[27] and the LLE and the VLE of several pyridinium-based ILs + alcohol systems.[28] Ferreira and colleagues[29,30] recently performed an extensive work concerning the application of the COSMO-RS to describe the phase equilibria of ionic liquid + hydrocarbon binary mixtures[29] and alkane + aromatic hydrocarbon + IL ternary systems.[30] Sistla and Khanna[31] used this same model to predict Henry's constants of carbon dioxide in several pyridinium-based ILs.

In the past few years, the statistical associating fluid theory (SAFT)[32,33] and, in particular, the soft-SAFT variant[34] have been shown to provide a physically grounded theoretical approach to describe the thermophysical properties and phase behavior of ILs and their mixtures in good agreement with the experimental data. The soft-SAFT equation of state was first applied for the modeling of ILs by Andreu and Vega[35] to successfully describe the solubility of CO_2 in 1-alkyl-3-methylimidazolium tetrafluoroborate ($[C_n\text{mim}][BF_4]$) and in 1-alkyl-3-methylimidazolium hexafluorophosphate ($[C_n\text{mim}]$-$[PF_6]$) ILs. They were represented by a simple model, as Lennard-Jones (LJ) chains containing one associating site representing the specific interactions between the cation and the anion as an ion pair. The same authors extended their approach to describe imidazolium-based ILs with the $[NTf_2]^-$ anion and the solubility behavior of CO_2, H_2, and Xe in some selected ILs.[36] In this case, this family of ILs was described as Lennard-Jones chains with three associating sites. The appearance of new experimental data allowed re-evaluating soft-SAFT results for this family of ILs and related mixtures with alkanols and water.[37] The modeling of the $[C_n\text{mim}][PF_6]$ family was also extended to describe the solubility of gases other than CO_2 and the mutual solubilities with water.[38,39] Finally, the ability of different imidazolium ILs to absorb acid gases (H_2S and SO_2) and ammonia (NH_3) for separation purposes was also very recently modeled with soft-SAFT.[40] All of these works show the ability of the soft-SAFT equation of state as a modeling tool to evaluate the thermophysical properties of ILs and their phase equilibria behavior with complex associating compounds.

In this work, the soft-SAFT equation of state is extended to the description of the family of ILs formed by a pyridinium cation and the bis[(trifluoromethyl)sulfonyl]imide anion. In particular, the study is focused on the 3-methyl-1-alkylpyr-

idinium bis[(trifluoromethyl)sulfonyl]imide ([$C_n$mpy][NTf_2]) and 1-alkylpyridinium bis[(trifluoromethyl)sulfonyl]imide ([$C_n$py][NTf_2]) series, and their mixtures with water, carbon dioxide, and sulfur dioxide.

This paper is organized as follows: after the theory section, a discussion about the most appropriate molecular model to describe the selected family of ILs is given, based on the most recent molecular simulation studies regarding their charge distribution and cation−anion interactions. With this information, it is possible to find an appropriate set of molecular parameters by fitting them to pure component liquid density experimental data at atmospheric pressure. Then, the established molecular model is tested by predicting the density behavior at high pressures and second-order thermodynamic derivative properties. The surface tension is also provided using the density gradient theory (DGT). Finally, the soft-SAFT EoS is applied to describe the solubility of carbon dioxide and sulfur dioxide, as well as the liquid−liquid equilibrium with water, in several pyridinium−bis[(trifluoromethyl)sulfonyl]imide ILs. A discussion about the selected molecular parameters considering their ability to describe these thermophysical properties is also presented.

2. THEORY

SAFT[32,33] is a very well-known theory coming from a first-order approximation of the perturbation theory of Wertheim[41,42] in which the different molecular effects on a system are separated and quantified. The soft-SAFT equation of state[34] is an accurate version of SAFT written, as all other versions, in terms of a sum of contributions to the total Helmholtz free energy of the system:[43,44]

$$a^{\mathrm{res}} = a - a^{\mathrm{id}} = a^{\mathrm{ref}} + a^{\mathrm{chain}} + a^{\mathrm{assoc}} + a^{\mathrm{polar}} \tag{1}$$

Each term of the above equation stands for different microscopic contributions to the total energy of the system. a^{res} is the residual Helmholtz free energy and a^{id} corresponds to the ideal contribution. Subsequently, ref, chain, assoc, and polar represent, in order of appearance, the reference term, the chain formation, the association, and the polar interactions.

In the soft-SAFT EoS, the reference term is a LJ spherical fluid which takes into account the repulsive and the attractive interactions of the monomers that constitute the chain. The reference term includes two molecular parameters representing the monomer: the segment diameter, σ_{ii}, and the dispersive energy between segments, ε_{ii}/k_B.[37] In our approach, the reference term is computed using the equation of Johnson et al.[45]

As there is not an expression of the reference term for mixtures, the van der Waals one-fluid theory with the modified Lorentz−Berthelot combining rules, given in eqs 2 and 3, is applied when the soft-SAFT is extended for mixtures:

$$\sigma_{ij} = \eta_{ij}\left(\frac{\sigma_{ii} + \sigma_{jj}}{2}\right) \tag{2}$$

$$\varepsilon_{ij} = \xi_{ij}(\varepsilon_{ii}\varepsilon_{jj})^{1/2} \tag{3}$$

with η_{ij} being the size and the ξ_{ij} energy binary parameters, accounting for size and energy asymmetries between the different components of the mixture, respectively. These values become one when using the equation in a predictive approach, from pure component parameters.

The chain and association terms derive directly from the Wertheim's first-order thermodynamic perturbation theory (TPT1):[41,42]

$$a^{\mathrm{chain}} = \rho k_B T \sum_i x_i(1 - m_i) \ln g_{\mathrm{LJ}} \tag{4}$$

$$a^{\mathrm{assoc}} = \rho k_B T \sum_i x_i \sum_\alpha \left(\ln X_i^\alpha - \frac{X_i^\alpha}{2}\right) + \frac{M_i}{2} \tag{5}$$

with ρ being the molecular density, T the temperature, m_i the chain length, x_i the molar fraction of component i, k_B the Boltzmann constant, and g_{LJ} the radial distribution function at density $\rho = m\rho_{\mathrm{monomer}}$ of LJ spheres, with ρ_{monomer} being the monomer density. The value of g_{LJ} is given by the fitted computer simulation data, as a function of density and temperature, proposed by Johnson et al.[46] X_i^α is the fraction of pure component i not bonded at site α and M_i the number of association sites of type α in component i. X_i^α is given by

$$X_i^\alpha = \frac{1}{1 + N_{\mathrm{av}}\rho \sum_j x_j \sum_\beta X_j^\beta \Delta_{\alpha\beta,ij}} \tag{6}$$

The specific site−site function, $\Delta_{\alpha\beta,ij}$, is described as

$$\Delta_{\alpha\beta,ij} = K_{\alpha\beta,ij} f_{\alpha\beta,ij} g_{ij}^{\mathrm{LJ}} \tag{7}$$

with $K_{\alpha\beta,ij}$ being related to the site−site bonding volume of association and the Mayer f-function:

$$f_{\alpha\beta,ij} = \left[\exp\left(\frac{\varepsilon_{\alpha\beta,ij}^{\mathrm{HB}}}{k_B T}\right) - 1\right] \tag{8}$$

The Mayer function includes the site−site association energy parameter $\varepsilon_{\alpha\beta}^{\mathrm{HB}}/k_B$.

The multipolar term for fluids of linear symmetrical molecules, such as CO_2, which are of interest for this work, accounts for the quadrupole−quadrupole interactions. This term is obtained using an extension of the theory of Gubbins and Twu[47] (originally developed for spherical molecules) to chain fluids, following the ideas of Jog et al.[48] The methodology is based in a perturbative approach of the Helmholtz free energy density due to the polarity effects. The free energy is expanded in a series of terms, written with the Padé approximation:[49]

$$a^{qq} = a_2^{qq}\left(1 - \frac{a_3^{qq}}{a_2^{qq}}\right)^{-1} \tag{9}$$

a_2^{qq} is the second-order term in the perturbation expansion, and a_3^{qq} is the third-order term. Expressions for a_2^{qq} and a_3^{qq} were obtained for an arbitrary intermolecular reference potential and involve state variables, molecular parameters, and the integral J for the reference fluid.[47] The previous expressions include the quadrupole moment, Q_i, of the molecule. Moreover, the extension to chain fluids assumes that the polar moments are well-localized on certain segments of the chain.[48] As a consequence, a fraction x_{pi} has to be defined as the fraction of the molecule affected by the quadrupole.

Within the soft-SAFT framework, non-self-associating molecules are defined by three molecular parameters: the chain length, m_i, the segment diameter, σ_{ii}, and the dispersive energy between segments, ε_{ii}/k_B. Linear symmetrical molecules with quadrupole involve the additional molecular parameters Q_i

dx.doi.org/10.1021/jp303166f | J. Phys. Chem. B 2012, 116, 9089−9100

Table 1. Molecular Weight and Optimized Molecular Parameters and for Carbon Dioxide,[62] Sulfur Dioxide,[40] and Water [61]

	M_w (g/mol)	m_i	σ_{ii} (Å)	ε_{ii}/k_B (K)	$\varepsilon_{ii}^{HB}/k_B$ (K)	K_{ii}^{HB} (Å^3)	Q (C m^2)
CO_2	44.01	1.571	3.184	160.2			4.40×10^{-40}
SO_2	64.06	2.444	2.861	228.3	1130	601	
H_2O	18.01	1.000	3.154	365.0	2388	2932	

and x_{pi}. For associating molecules two more parameters are included to model the associating interactions: the site−site association energy, $\varepsilon_{\alpha\beta,ij}^{HB}/k_B$, and the site−site bonding volume of association, $K_{\alpha\beta,ij}$.

The density gradient theory was coupled with the soft-SAFT equation to compute interfacial properties. DGT was first proposed by van der Waals[50] and then re-discovered by Cahn and Hilliard.[51]

The expression for the Helmholtz energy of the system is given by

$$A = \int \left[a_0(\rho) + \sum_i \sum_j \frac{1}{2} c_{ij} \nabla\rho_i \nabla\rho_j \right] d^3r \tag{10}$$

where $a_0(\rho)$ is the Helmholtz free energy density of the homogeneous fluid at the local density ρ and ρ_i is the molar density of component i. c_{ij} is the influence parameter that is assumed to be temperature independent. Its value is normally regressed from interfacial tension experimental data.

Assuming a planar interface and neglecting the c_{ij} density dependence, it is possible to derive an expression relating interfacial tensions and the square of the density gradient:[52]

$$\gamma = \sum_i \sum_j \int_{-\infty}^{+\infty} c_{ij} \frac{d\rho_i}{dz} \frac{d\rho_j}{dz} dz = 2 \int_{-\infty}^{+\infty} [a_0(\rho) - \sum_i \rho_i \mu_{0i} - p_0] dz \tag{11}$$

where μ_{0i} and p_0 are the equilibrium chemical potential and pressure, respectively, and z is the direction perpendicular to the interface. Further details about the implementation of the DGT approach into soft-SAFT can be found in previous works.[53−55]

3. MOLECULAR MODEL

When modeling an associating compound, the choice of an appropriate association scheme to represent the main physical short-range interactions is vital for an accurate description of its thermodynamic properties. For the particular case of ILs, previous efforts had already been considered to model imidazolium-based ILs with soft-SAFT.[35−40] As explained in these papers, the anions and cations forming ILs are considered to be together as ion pairs, based on experimental and theoretical studies.[56,57] In addition, specific associating sites can be used to represent interactions between counterions, since studies have proven that bulky size and ions asymmetric charge distribution soften Coulomb forces generating short-range highly directional interactions.[58] Recent work[59] also shows that dispersion forces, specific steric interactions, and short-lived ion pairs reduce the ionic character of these compounds.

Using this information, and considering the fact that the $[C_npy][NTf_2]$ ILs have a charge distribution similar to those of $[C_nmim][NTf_2]$ ILs,[60] we have transferred the same molecular model utilized for the imidazolium ILs with the $[NTf_2]$ anion to the pyridinium ILs with the same anion. Consequently, pyridinium$[NTf_2]$ ILs are considered as a chain of LJ monomers of diameter σ_{ii} and dispersive energy ε_{ii}/k_B with three associating sites to represent anion−cation interactions: one A type associating site represents the nitrogen atom interactions with the cation, and two B sites represent the delocalized charge due to the oxygen molecules on the anion, allowing only AB interactions between different ionic liquid molecules.

The rest of the molecules considered in this work have already been modeled in previous contributions, and we use them in a transferable manner in this work. Water (H_2O)[37,61] is considered to be a single spherical LJ monomer $(m_{H_2O} = 1)$ with four associating sites, in which hydrogen bonding is considered to occur between the two hydrogen atoms and the two lone pairs of electrons in the oxygen of the water molecules. Carbon dioxide (CO_2)[62] is modeled as a LJ chain in which explicit quadrupolar interactions are taken into account. Consequently, in addition to the molecular parameters described above, it also requires the quadrupole moment, Q, and x_p, the fraction of segments in the chain that contains the quadrupole. x_p was fixed to 1/3 to mimic molecules as three segments with a quadrupole in one of them. The effective quadrupole moment for CO_2, obtained from fitting, was within the range of the values found in the literature.[63,64] Finally, sulfur dioxide (SO_2) is represented by a LJ chain with two associating sites of different nature (positive−negative) to mimic in an effective manner the nature of the dipole moment of the molecule,[40] in an approach similar to that done in a previous work to represent the dipole moment of hydrogen chloride.[65] The molecular parameters for H_2O, CO_2, and SO_2 have been taken from previous contributions,[40,61,62] and more details of each one of these models can be found in the original references; the parameters are summarized in Table 1 for completeness.

4. RESULTS AND DISCUSSION

The ILs included in this study correspond to the series of 1-alkyl-3-methylpyridinium and 1-alkylpyridinium with the bis-(trifluoromethylsulfonyl)imide anion ($[C_nmpy][NTf_2]$ with n = 2, 3, 4, 6, 8 and $[C_npy][NTf_2]$ with n = 2, 3, 4, 5, 6, 8, 10, 12).

4.1. Thermophysical Properties of Pure Pyridinium ILs. Once the molecular model and, in particular, the association scheme have been decided, the molecular parameters of each ionic liquid are fitted to liquid density data at atmospheric pressure. From a numerical perspective, the optimization of five molecular parameters allows an important amount of combinations with small deviations from the experimental density. Hence, we apply here successive assumptions based on physical arguments, previous experience, and the transferability of the soft-SAFT molecular parameters for similar compounds, in order to reduce the number of solutions, and to use the soft-SAFT approach in a way as transferable as possible.

Due to the similarity between $[NTf_2]^-$ pyridinium and imidazolium ILs in chemical structure and size, a first assumption was to keep for the pyridinium ionic liquid the

dx.doi.org/10.1021/jp303166f | J. Phys. Chem. B 2012, 116, 9089−9100

Table 2. Molecular Weight, Optimized Molecular Parameters, and Absolute Average Deviation (AAD) for the Densities of the $[C_n mpy][NTf_2]$ and $[C_n py][NTf_2]$ Series[a]

	M_w (g/mol)	m_i	σ_{ii} (Å)	ε_{ii}/k_B (K)	ε^{HB}/k_B (K)	K_{ii}^{HB} (Å^3)	AAD%
$[C_2\ mpy][NTf_2]$[b,76]	402.33	6.023	4.125	418.0	1550	2020	0.06
$[C_3\ mpy][NTf_2]$ [68]	416.37	6.101	4.194	418.0	1550	2020	0.04
$[C_4\ mpy][NTf_2]$ [68]	430.39	6.175	4.257	418.0	1550	2020	0.14
$[C_6\ mpy][NTf_2]$ [66]	458.44	6.338	4.375	418.0	1550	2020	0.08
$[C_8\ mpy][NTf_2]$[b,75]	486.49	6.489	4.483	418.0	1550	2020	2.29
$[C_2py][NTf_2]$[b,71]	388.30	5.947	4.044	418.0	1550	2020	0.51
$[C_3py][NTf_2]$ [72]	402.33	6.023	4.119	418.0	1550	2020	0.03
$[C_4py][NTf_2]$ [69]	416.37	6.101	4.193	418.0	1550	2020	0.03
$[C_5py][NTf_2]$ [67]	430.38	6.175	4.248	418.0	1550	2020	0.09
$[C_6py][NTf_2]$ [68]	444.42	6.247	4.305	418.0	1550	2020	0.13
$[C_8py][NTf_2]$ [68]	472.48	6.418	4.429	418.0	1550	2020	0.06
$[C_{10}py][NTf_2]$ [70]	500.52	6.575	4.529	418.0	1550	2020	0.07
$[C_{12}py][NTf_2]$[b,70]	528.57	6.732	4.622	418.0	1550	2020	0.21

[a]References include the sources of experimental data. [b]The molecular parameters of these compounds are predicted with the correlations proposed in eq 12-13

same value for the chain molecular parameter, m_i, as that of the correspondent imidazolium ionic liquid, i.e., having the same number of carbons in the alkyl chains substitutions on the cation ring.[37] Here, it is interesting to note the difference between the $[C_n mpy][NTf_2]$ and $[C_n py][NTf_2]$ families. While the first family is analogous to the $[C_n mim][NTf_2]$ and the values are directly transferred (i.e., $m_{[C_4mpy][NTf_2]} = m_{[C_4mim][NTf_2]}$), the second one lacks the methyl group. Hence, the values transferred correspond to $[C_{n-1}mim]$ (i.e., $m_{[C_4py][NTf_2]} = m_{[C_3mim][NTf_2]}$). The other four parameters were obtained by fitting to experimental data[66−72] of the temperature−density diagram at atmospheric pressure.

An additional constraint was imposed for the site−site association energy $\varepsilon_{\alpha\beta,ij}^{HB}/k_B$ and the site−site bonding volume of association $K_{\alpha\beta,ij}$. As done for other ILs modeled with soft-SAFT,[35−40] it was assumed that the associating interactions are independent of the alkyl-chain length of the cation and are assumed to be constant for all of the members of the same family. Since the relative cation−anion interaction strengths are lower for $[NTf_2]^-$ pyridinium ILs (lower experimental dissociation energies),[73] lower values for the association molecular parameters than the ones obtained for $[NTf_2]^-$ imidazolium ILs are also expected.

The parameters regression was done first for the $[C_3mpy][NTf_2]$ ionic liquid, chosen as a case study because of the important amount of experimental data available. The fitting provided a site−site association energy, $\varepsilon_{\alpha\beta,ij}^{HB}/k_B$, value of 1550 K and a site−site bonding volume of association, $K_{\alpha\beta,ij}$, of 2020 Å^3. Then, those values were assumed constant for all of the selected $[NTf_2]$ pyridinium ILs, and the remaining two molecular parameters σ_{ii} and ε_{ii}/k_B were fitted to the experimental density data for the rest of them. Even with all of these restrictions, there were some sets of molecular parameters still providing a good description of the liquid density at atmospheric pressure. To discriminate among values, the surface tension was calculated for some of the members for which there were available experimental data ($[C_3mpy][NTf_2]$,[74] $[C_4py][NTf_2]$,[67] and $[C_5py][NTf_2]$[67]). Here, it is important to remark that the DGT procedure involved the additional influence parameter c_{ii}. Then, once a possible set of parameters was found to reproduce the temperature−density diagram, the c_{ii} parameter was later fitted to surface tension.

From these calculations, it was possible to identify the dispersive energy ε_{ii}/k_B as the most influent parameter for better reproducing the slope of the surface tension with the temperature. In general terms, similar values were obtained for each ionic liquid. Hence, a third restriction was to fix a constant average value of ε_{ii}/k_B = 418 K for all the members of the pyridinium family, leaving only σ_{ii} as a fitting variable. In that way, it was possible to find a very simple and transferable model, with three constant parameters for all the selected compounds, and a fourth one transferred from another family. With all these considerations in mind, a final set of molecular parameters for the selected pyridinum ILs studied in this work was found. These values are presented in Table 2.

With the selected parameters, an excellent description of the density−temperature diagram was obtained (Figure 1) for the $[C_n py][NTf_2]$ (n = 3−10) and $[C_n mpy][NTf_2]$ (n = 3−6) ILs,

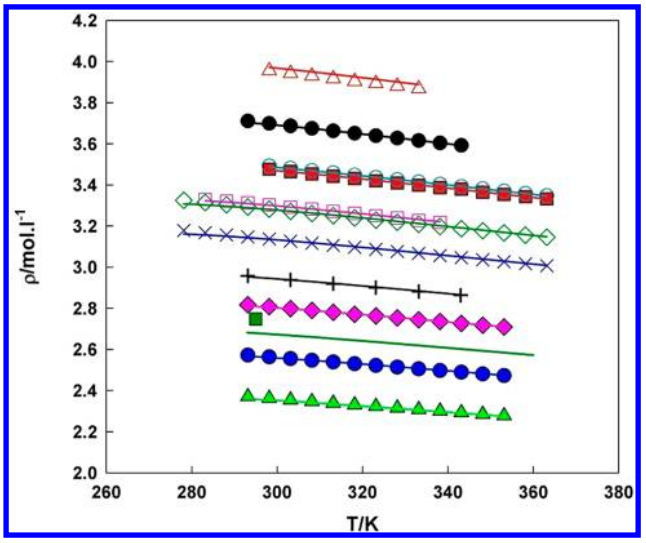

Figure 1. Temperature−density diagram for $[C_n mpy][NTf_2]$ and $[C_n py][NTf_2]$, at atmospheric pressure. Symbols represent experimental data[66−72] (●, $[C_2mpy][NTf_2]$; red ■, $[C_3mpy][NTf_2]$; ◊, $[C_4mpy][NTf_2]$; +, $[C_6mpy][NTf_2]$; green ■, $[C_8mpy][NTf_2]$; Δ, $[C_2py][NTf_2]$; ○, $[C_4py][NTf_2]$; □, $[C_5py][NTf_2]$; × , $[C_6py][NTf_2]$; pink ♦, $[C_8py][NTf_2]$; blue ●, $[C_{10}py][NTf_2]$; light green ▲, $[C_{12}py][NTf_2]$) and the lines soft-SAFT results.

dx.doi.org/10.1021/jp303166f | J. Phys. Chem. B 2012, 116, 9089−9100

with global average deviations inferior to 0.20% in density. As previously observed for imidazolium ILs,[37] it is possible to establish a trend between the m_i and σ_{ii} molecular parameters and the molecular weight (M_w), following a linear dependency. However, it is important to distinguish between the $[C_npy][NTf_2]$ and the $[C_nmpy][NTf_2]$ compounds. Although they are of very similar nature, the presence of an extra methyl group slightly modifies their properties. As the chain length parameter m_i is transferred for all compounds from the imidazolium according to the number of carbons in the radicals of the cation, no formal differences are considered for this parameter. As a consequence, the size/volume differences are accounted for solely by the segment diameter values σ_{ii}. If an only correlation were given, all the compounds with the same molecular weight (see, for instance, $[C_3mpy][NTf_2]$ and $[C_4py][NTf_2]$) would have exactly the same parameters. Hence, it is necessary to have a different correlation for the segment diameter σ_{ii} to account for this small difference:

$$m_i\sigma_{ii}^3 = 1.9345M_w - 357.92\ (\text{Å}^3)\quad (\text{for the } [C_npy][NTf_2] \text{ family}) \tag{12}$$

$$m_i\sigma_{ii}^3 = 1.9205M_w - 349.81\ (\text{Å}^3)\quad (\text{for the } [C_nmpy][NTf_2] \text{ family}) \tag{13}$$

The use of a constant value for ε_{ii}/k_B, $K_{\alpha\beta,ij}$, $\varepsilon_{\alpha\beta,ij}^{HB}/k_B$, the transferability of m_i and the correlation of σ_{ii} allow the soft-SAFT EoS to be used in a predictive manner for other compounds of the same family. For that reason, the previous correlations only included compounds from $[C_3py][NTf_2]$ until $[C_{10}py][NTf_2]$ and from $[C_3mpy][NTf_2]$ until $[C_6mpy][NTf_2]$. The molecular parameters of lower and higher alkyl chain lengths have been predicted (σ_{ii} values were computed from the correlations given in eqs 12 and 13, and m_i values were transferred from the imidazoliums according to the number of carbons in the radicals of the cation). In the same Figure 1, the temperature−density diagrams of $[C_2py][NTf_2]$, $[C_{12}py][NTf_2]$, $[C_2mpy][NTf_2]$, and $[C_8mpy][NTf_2]$ are provided as predictions using soft-SAFT with the correlations, with very good agreement in all cases, excepting for the single data point of $[C_8mpy][NTf_2]$. Unfortunately, the fact that there is only one single experimental point[75] does not allow one to provide conclusions. In the other three cases, the predictions are in very good agreement with the experimental data[70,71,76] as also observed in Table 2.

In Figure 2, the surface tension of the four ILs ($[C_3mpy][NTf_2]$, $[C_2py][NTf_2]$, $[C_4py][NTf_2]$, and $[C_5py][NTf_2]$) with available experimental data is presented. Once the set of molecular parameters for phase calculations is established, the influence parameter c_{ij} was fitted to these data for each compound, reaching good agreement in all cases, with an AAD % = $(1/N)\Sigma_{i=1}^{n}((\gamma_{expt} - \gamma_{calc})/\gamma_{expt}) \times 100$ of less than 0.60%, which is within the experimental uncertainty. As done for the $[C_nmim][Tf_2N]$ family,[37] it was possible to identify a trend between the influence parameter and the molecular weight of the members of the $[C_npy][Tf_2N]$ series. However, surface tension experimental data for more pyridinium ILs of this type are still needed to confirm any tendency. A summary of the influence parameter values and the global average deviations for the soft-SAFT + DGT results are shown in Table 3.

In addition, the vapor−liquid phase envelope of all of the compounds has been calculated. Even if there are no

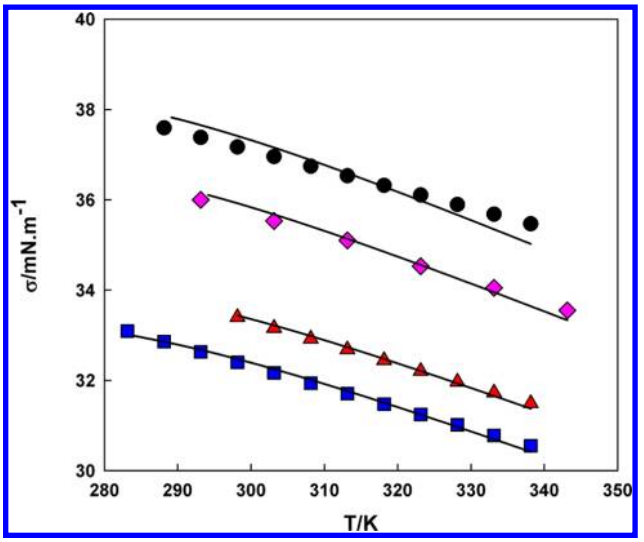

Figure 2. Surface tensions for $[C_nmpy][NTf_2]$ and $[C_npy][NTf_2]$. Symbols represent experimental data[67,74] (●, $[C_2py][NTf_2]$; ▲, $[C_4py][NTf_2]$; ■, $[C_5py][NTf_2]$; ♦, $[C_3mpy][NTf_2]$) and the lines soft-SAFT results.

Table 3. Optimized Influence Parameter for $[C_nmpy][NTf_2]$ and $[C_npy][NTf_2]$ Compounds and Modeling Results for Surface Tensions[a]

compound	$10^{19}c$ (J m^5 mol^{-2})	AAD%
$[C_2py][NTf_2]$ [67]	16.32	0.58
$[C_4py][NTf_2]$ [67]	18.45	0.16
$[C_5py][NTf_2]$ [67]	20.55	0.26
$[C_3mpy][NTf_2]$ [74]	21.89	0.36

[a]References include the sources of experimental data.

experimental data to compare, it is interesting to check if the critical properties, the vapor pressure or the enthalpy of vaporization, are within the same order of magnitude as other similar ILs. The calculations (not shown here) have provided typical values for ILs, with critical temperatures between 1100 and 1200 K, near-zero vapor pressures (10^{-8}−10^{-9} Pa at 300 K) and enthalpies of vaporization around 80 and 85 kJ/mol at boiling temperature.

One of the goals of this work is to propose a molecular model for these systems with a high degree of accuracy and transferability, physically sounded. Even if several important assumptions have been made, the main physical interactions of the molecule should be kept in the model. Hence, the chosen set of molecular parameters are now used to calculate in a predictive manner the density of the ILs at high pressures, as well as some second-order thermodynamic derivative properties. In particular, the evaluation of derivative properties of those ILs is important for practical applications. Furthermore, they constitute a very stringent test in order to determine the accuracy of the underlying molecular model and the capabilities of the equation of state.[37] Unfortunately, to our knowledge, there are no direct experimental data measured, and only comparison with derivative properties data calculated through indirect methods can be made.

Gardas et al.[77] presented experimental values for the pressure dependency at different temperatures of the $[C_3mpy][NTf_2]$ density along with the derivative thermodynamic properties obtained with the Tait equation, such as the isothermal compressibility (κ_T). The density of several $[C_3mpy][NTf_2]$

dx.doi.org/10.1021/jp303166f | J. Phys. Chem. B 2012, 116, 9089−9100

isotherms in a range of pressures up to 35 MPa was calculated with soft-SAFT and compared with these data[77] in Figure 3. An

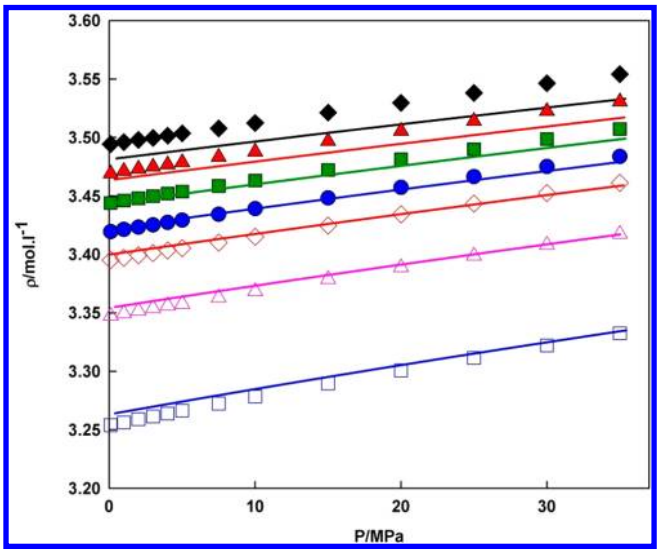

Figure 3. Pressure−density diagram for $[C_3mpy][NTf_2]$. Symbols stand for experimental data[77] (♦; 293.15 K; ▲, 303.15 K; ■, 313.15 K; ●, 323.15 K; ◊, 333.15 K; Δ, 353.15 K; □, 393.15 K) and the lines for soft-SAFT predictions.

excellent prediction of the density−pressure dependence was obtained with the equation, showing that the model is valid to evaluate the density at high pressures. Then, in Figure 4, the

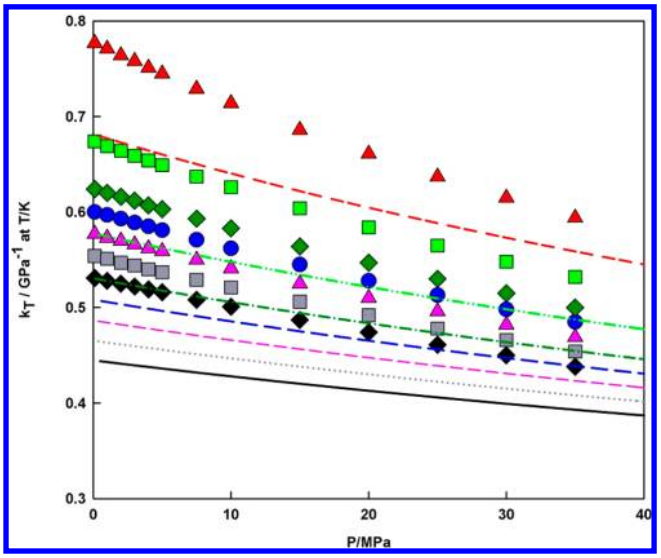

Figure 4. Isothermal compressibility for $[C_3mpy][NTf_2]$. Symbols stand for calculated data from the Tait equation fitted to experimental densities[77] (♦; 293.15 K; ■, 303.15 K; ▲, 313.15 K; ●, 323.15 K; ♦, 333.15 K; ■, 353.15 K; ▲, 393.15 K) and the lines for soft-SAFT predictions.

isothermal compressibility (κ_T) predictions are depicted. These properties are slightly underpredicted by the soft-SAFT EoS, although qualitative agreement is found, following the right trend in the whole range of temperatures.

4.2. CO_2 and SO_2 Solubility in $[C_npy][NTf_2]$ and $[C_nmpy][NTf_2]$. The solubility of gases in ILs is of clear importance in the search of selective compounds for gas separation, carbon capture, and supercritical fluids applications using ILs. A detailed description of the solubility of gases and supercritical fluids in $[C_nmpy][NTf_2]$ and $[C_npy][NTf_2]$ is of major importance for a further understanding and improvement of these processes.[78]

The soft-SAFT model for the pyridinium-based ILs developed in this work is used here to model the CO_2 and SO_2 solubilities on those ILs. Experimental information was available for CO_2 in four $[C_npy][NTf_2]$ ILs,[79] (n = 4, 8, 10, 12), and two $[C_nmpy][NTf_2]$ ILs[80,81] (n = 4, 6), and for SO_2 in $[C_6mpy][NTf_2]$.[82]

For the case of carbon dioxide, no explicit associating interactions between the ILs and the CO_2 are taken into account, as the quadrupole effect of CO_2 has already been specifically accounted for. Conversely, the selected molecular model for SO_2 allows the possibility of considering cross-association between the sites of SO_2 and those of the ionic liquids. Hence, we have applied the same assumptions done when studying the solubility of SO_2 in imidazolium $[NTf_2]$ ionic liquids[40] and have considered interactions between the positive site of SO_2 (site +) and the two B sites of the ionic liquid (+B) and between the negative site of SO_2 (site −) and the site A of the ionic liquid (−A). In all those mixtures, as done previously,[35−40,62] the differences in energy of the segments forming the chain are accounted for with the energy binary parameter, ξ_{ij}, while the unlike size binary parameter is calculated using the Lorentz combining rule without any fitting (η_{ij} = 1), i.e., only one binary parameter, related to energy is fitted, when needed.

We have first studied the CO_2 solubility in $[C_npy][NTf_2]$ ILs. The phase diagram of CO_2 + $[C_4py][NTf_2]$ at three temperatures in the range of 298.15 until 333.15 K is presented in Figure 5a. The predicted solubility (without the use of any binary parameter) is in very good agreement with the experimental data[79] at all temperatures. Good results are achieved, even at higher pressures, as shown in Figure 5b for the same mixture at 298.15 K and a wider range of pressures. The solubility of CO_2 in $[C_8py][NTf_2]$ and $[C_{10}py][NTf_2]$ has also been modeled, and an isotherm at 298.15 K is presented in Figure 5c. Here, the predicted solubilities were higher than the experimental measurements.[79] As a consequence, an adjustable ξ_{ij} binary parameter has been fitted to mixture data, following the same patterns established to model the solubility of CO_2 in imidazolium $[NTf_2]$ ILs.[36] ξ_{ij} values of 0.950 for $[C_8py][NTf_2]$ and of 0.930 for $[C_{10}py][NTf_2]$ were found to provide good agreement with the experimental data. It is interesting to note that the ξ_{ij} value used to describe CO_2 + $[C_8mim][NTf_2]$ mixture in previous work[36] is exactly the same used here for $[C_8py][NTf_2]$ IL. This feature allows the thought that the nature of the interactions of CO_2 with the pyridinium $[NTf_2]$ family is very similar than that for the imidazolium $[NTf_2]$ family and gives confidence about the assumptions made when optimizing the pure ILs.

In Figure 6, we have modeled the CO_2 solubility in two $[C_nmpy][NTf_2]$ compounds, for which experimental data were available. In Figure 6a, the mixture CO_2 + $[C_4mpy][NTf_2]$ at atmospheric pressure was shown in a composition−temperature diagram. In this case, a ξ_{ij} value of 0.985 was found to provide a good description of the phase equilibrium diagram. This value is quite close to 1 and, again, similar to the one used in the previous description of CO_2 + $[C_4mim][NTf_2]$ (ξ_{ij} = 0.972).[37] In addition, the CO_2 solubility on $[C_6mpy][NTf_2]$ at three temperatures in the range of 283−323 K is presented in

dx.doi.org/10.1021/jp303166f | J. Phys. Chem. B 2012, 116, 9089−9100

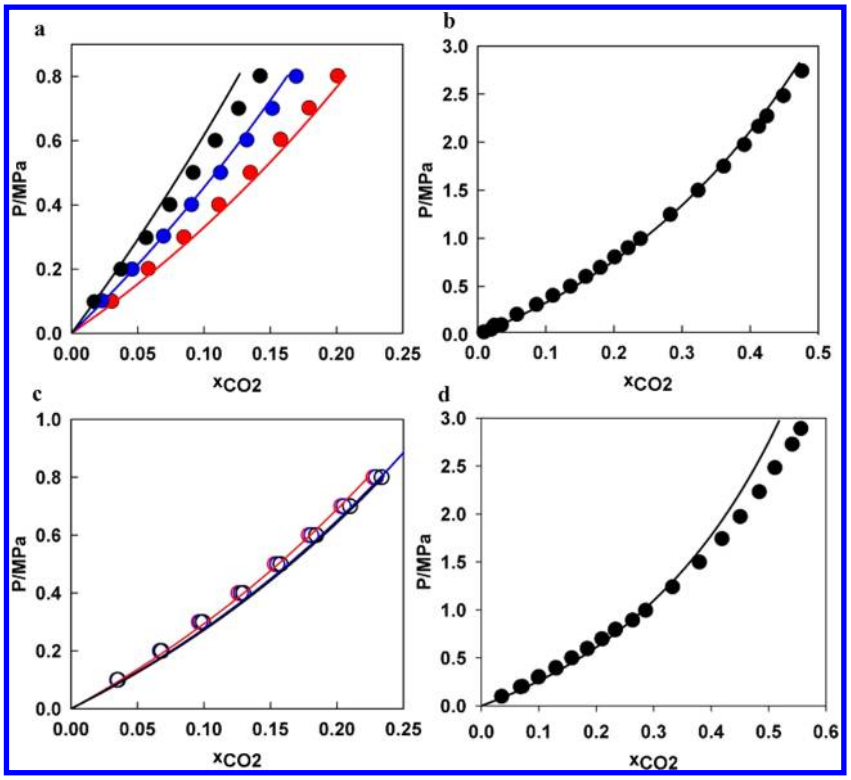

Figure 5. (a) CO_2 solubility in $[C_4py][NTf_2]$. Symbols stand for experimental data[79] (red ●, 298.15 K; blue ●, 313.15 K; black ●; 333.13 K) and the lines for soft-SAFT prediction results using binary interaction parameters equal to 1. (b) CO_2 solubility in $[C_4py][NTf_2]$ at 298.15 K. Symbols stand for experimental and the lines for soft-SAFT prediction results using binary interaction parameters equal to 1. (c) CO_2 solubility in $[C_npy][NTf_2]$. Symbols stand for experimental data[79] (red ○, $[C_8py][NTf_2]$; blue ○, $[C_{10}py][NTf_2]$; black ○, $[C_{12}py][NTf_2]$) and the lines for soft-SAFT results (ξ_{ij} of 0.950 for $[C_8py][NTf_2]$, ξ_{ij} of 0.930 for $[C_8py][NTf_2]$, and ξ_{ij} of 0.915 for $[C_{12}py][NTf_2]$). (d) CO_2 solubility in $[C_{12}py][NTf_2]$ at 298.15 K. Symbols stand for experimental results and the lines for soft-SAFT results using a ξ_{ij} of 0.915.

Figure 6b. A temperature-independent energy parameter ξ_{ij} = 0.960 was adjusted at the intermediate temperature of 298 K. Then, the other two isotherms were predicted using the same binary parameter, with excellent agreement with the experimental data.[81] Once again, the comparison with the molecular model of the equivalent imidazolium ionic liquid $[C_6mim][NTf_2]$ with CO_2 reveals a similar value (ξ_{ij} = 0.948).[36]

From the previous results, it is evident that the longer the alkyl chain of the cation is, the more deviations from predictions are observed. In other words, our model is not sufficiently considering that the increase of the alkyl chain decreases the solubility of CO_2 and we have to correct it by adjusting the ξ_{ij}. This is not a shortcut of the model used for the ILs or CO_2, but it is related to the van der Waals one fluid theory used for the mixtures, given the fact that the compounds of the mixture become more asymmetric in length. The binary parameter corrects this asymmetry, as it does for asymmetric mixtures as simple as hydrocarbons.[83,84] However, the observation of the values found shows a clear trend that can be related with the molecular weight of the IL. The plot of the values of ξ_{ij} with the molecular weight for $[C_4py][NTf_2]$, $[C_8py][NTf_2]$, $[C_{10}py][NTf_2]$, $[C_4mpy][NTf_2]$, and $[C_6mpy][NTf_2]$ in Figure 7 reveals this tendency. Since one of our goals is to keep the procedure as predictive as possible, we can identify a second-order polynomial correlation that will allow one to predict the parameter of other mixtures of the same family:

$$\xi_{ij} = 2.586 \times 10^{-6} M_w^{\ 2} - 3.196 \times 10^{-3} M_w + 1.882 \quad (14)$$

In this case, we have not observed substantial differences between the $[C_npy][NTf_2]$ and $[C_nmpy][NTf_2]$ families and have plotted all of the parameters together. We have tested the validity of this correlation predicting the solubility of CO_2 in $[C_{12}py][NTf_2]$. The predictions at 298.15 K can be seen in Figure 5c (black line, for low pressures) and Figure 5d (high pressures). They are in good agreement with the experimental data[79] although some deviations are found at CO_2 compositions higher than 0.40. Otherwise, it is good to see how this predictive approach (pure $[C_{12}py][NTf_2]$ IL parameters and the binary parameter coming from predictions) provides a good description of the mixture.

Experimental data related to the SO_2 solubility in pyridiniums $[NTf_2]$ ILs are much scarcer, as only data for one mixture were found. The SO_2 + $[C_6mpy][NTf_2]$ mixture at 298.15 K (Figure 8) was successfully described using a ξ_{ij} value of 0.900, regressed from the experimental data,[82] as depicted in Figure 8. This value is very similar to that obtained for the SO_2 solubility in $[C_6mim][NTf_2]$ in a previous work (ξ_{ij} = 0.910),[40] showing once more the similarities between the pyridinium and imidazolium ILs.

4.3. LLE of H_2O + $[C_nmpy][NTf_2]$ and $[C_npy][NTf_2]$. An accurate description of the mutual solubilities between ILs and water is essential for extraction purposes and also for managing their ecological impact, since even the most hydrophobic ILs present some miscibility with water with possible secondary aquatic environmental risks.[85]

In this section, the capability of the proposed soft-SAFT model to describe the solubility of pyridinium-based ILs in water is shown. For comparison, experimental data were found

dx.doi.org/10.1021/jp303166f | J. Phys. Chem. B 2012, 116, 9089−9100

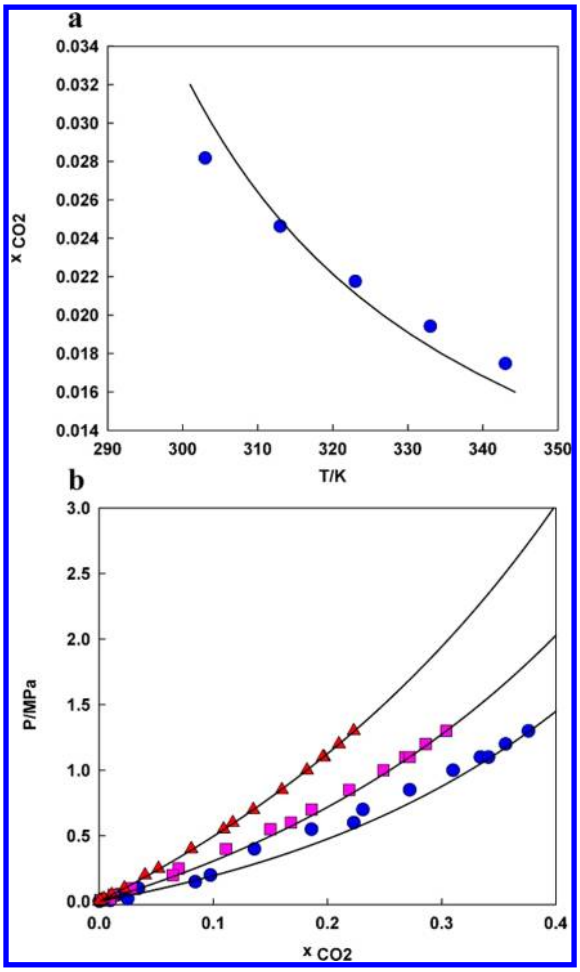

Figure 6. (a) CO_2 solubility in $[C_4mpy][NTf_2]$ at atmospheric pressure. Symbols stand for experimental data[80] and lines for the soft-SAFT results using a ξ_{ij} of 0.985. (b) CO_2 solubility in $[C_6mpy][NTf_2]$. Symbols stand for experimental data[81] (●, 283.17 K; ■, 298.17 K; ▲, 323.16 K) and lines for the soft-SAFT results using a ξ_{ij} of 0.960.

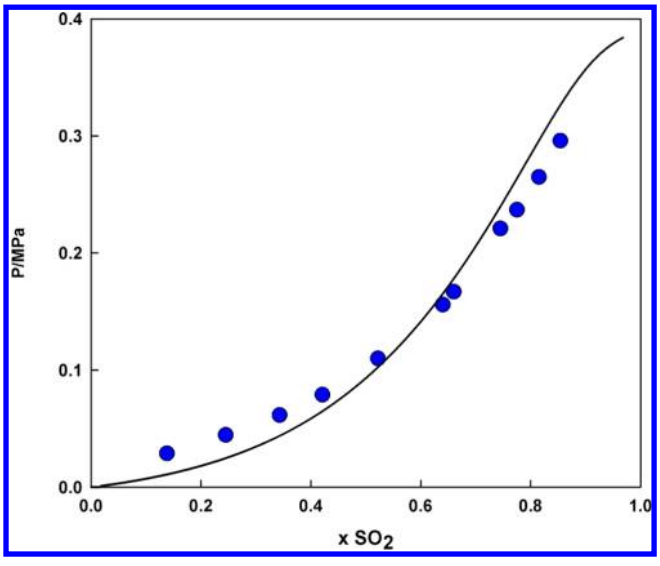

Figure 7. ξ_{ij} dependence with the molecular weight for $[C_nmpy][NTf_2]$ (blue ●) and for $[C_npy][NTf_2]$ (black ●).

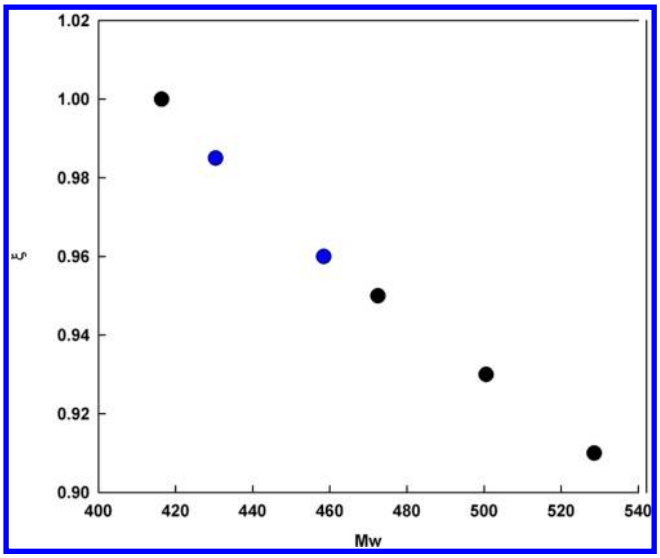

Figure 8. SO_2 solubility in $[C_6mpy][NTf_2]$ at 298.15 K. Symbols stand for experimental data[82] and lines for the soft-SAFT results using a ξ_{ij} of 0.90.

in the bibliography for aqueous binary systems containing $[C_4py][NTf_2]$, $[C_6py][NTf_2]$, $[C_8py][NTf_2]$, $[C_3mpy][NTf_2]$, and $[C_4mpy][NTf_2]$.[60]

Cross-association between water and the pyridinium-based ILs is explicitly taken into account using the Lorentz−Berthelot combining rules within the soft-SAFT framework, as previously done when modeling water + imidazolium-based ionic liquid systems.[37] Interactions can occur between the two B sites on the oxygen molecules of the anion and the two H sites on the hydrogen atoms of the water molecule, and between the A site on the nitrogen of the anion and the two e sites on the oxygens of the water molecule. Association volume and strength are the same for Ae and BH associations, and AH and Be interactions are set to zero.

The description of the liquid−liquid equilibria (LLE) of water with several pyridinium $[NTf_2]$ ILs is shown in Figure 9. In a previous work where the soft-SAFT was applied to water + $[NTf_2]$ imidazolium systems,[37] two adjustable binary parameters were required to achieve quantitative agreement with the experimental data. Here, only one binary parameter, η_{ij}, was necessary to improve the soft-SAFT description of the LLE of these systems. The other binary parameter (ξ_{ij}) is set to one. The procedure to find the binary size adjustable parameter, η_{ij}, consists of fitting to experimental data of the water-rich phase. Then, the value optimized was used to predict the ionic liquid rich phase solubility.

In Figure 9a, the mutual solubilities of $[C_4py][NTf_2]$, $[C_6py][NTf_2]$, $[C_8py][NTf_2]$, $[C_3mpy][NTf_2]$, and $[C_4mpy][NTf_2]$ with water are shown. The soft-SAFT calculations (lines) have been done using η_{ij} values, ranging from 0.70 to 0.75, providing an excellent agreement with the experimental data.[60] This range of values is similar to the binary adjustable parameter optimized for $C_nmim[PF_6]$ + water mixtures (η_{ij} = 0.695).[39] As stated in that publication, ILs have a molecular volume significantly higher than water, and a value of η_{ij} lower than 1 means that the intermolecular size of interaction is decreased. This behavior had already been observed in modeling the mutual solubilities of water with hydrocarbons,[61] confirming the idea that some ILs have an alkane-like behavior. A linear correlation for the binary interaction parameter with

dx.doi.org/10.1021/jp303166f | J. Phys. Chem. B 2012, 116, 9089−9100

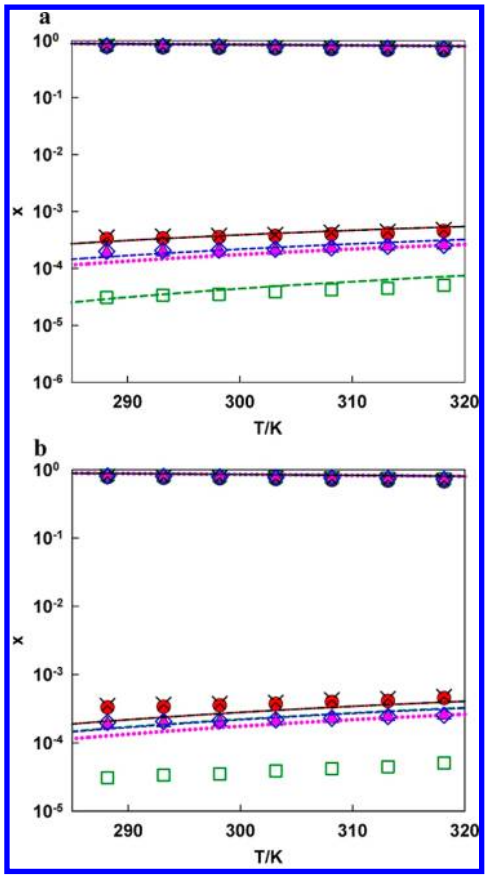

Figure 9. (a) LLE for $[C_n\text{mpy}][NTf_2]/[C_n\text{py}][NTf_2]$ + water systems. Symbols represent experimental data[56] (○, $[C_4\text{py}][NTf_2]$; Δ, $[C_6\text{py}][NTf_2]$; □, $[C_8\text{py}][NTf_2]$; ◊, $[C_4\text{mpy}][NTf_2]$; ×, $[C_3\text{mpy}][NTf_2]$) and lines the soft-SAFT results using an optimized value for the size binary parameter, η_{ij}, for each system ($[C_3\text{mpy}][NTf_2]$ + water η_{ij} = 0.70; $[C_4\text{mpy}][NTf_2]$ + water η_{ij} = 0.72; $[C_4\text{py}][NTf_2]$ + water η_{ij} = 0.70; $[C_6\text{py}][NTf_2]$ + water η_{ij} = 0.72; $[C_8\text{py}][NTf_2]$ + water η_{ij} = 0.75) (—, $[C_4\text{py}][NTf_2]$; ..., $[C_6\text{py}][NTf_2]$; — —, $[C_8\text{py}][NTf_2]$; --, $[C_4\text{mpy}][NTf_2]$; —·—, $[C_3\text{mpy}][NTf_2]$). (b) LLE for $[C_n\text{mpy}][NTf_2]/[C_n\text{py}][NTf_2]$ + water. Symbols represent experimental data[56] and lines stand for the soft-SAFT results using a constant value for the size binary parameter, η_{ij} = 0.72, for all systems. See text for details.

the molecular weight was also found for the selected pyridinium $[NTf_2]$ ILs (here, again, no substantial differences between $[C_n\text{py}][NTf_2]$ and $[C_n\text{mpy}][NTf_2]$ families were found), although the trend should be confirmed when more LLE experimental data for heavier ILs is available.

$$\eta_{ij} = 8.53 \times 10^{-4} M_w + 3.46 \times 10^{-1} \quad (15)$$

A final test was done by keeping a constant η_{ij} value of 0.72 for all the mixtures, in order to avoid a dependence on the molecular weight. As expected, higher deviations between the experimental and the soft-SAFT results were obtained, but still good agreement was found, as shown in Figure 9b, except for $C_8\text{py}[NTf_2]$, where a higher deviation was obtained. The observation of the experimental data[60] reveals that the solubility of this compound in water decreases drastically (1 order of magnitude) compared to the rest of compounds. In other words, the difference between the solubility in water of $C_4\text{py}[NTf_2]$ and $C_6\text{py}[NTf_2]$ is far less than the difference from $C_6\text{py}[NTf_2]$ to $C_8\text{py}[NTf_2]$. Hence, a constant η_{ij} value is not enough to account for that change of solubility.

5. CONCLUSIONS

The capability of the soft-SAFT EoS to describe the thermodynamic properties and phase behavior of pure ILs and their mixtures with water and gases, previously shown for imidazolium-based ILs, was extended in this work for $[NTf_2]$ pyridinium ILs.

On the basis of molecular simulation works, where a similar charge distribution between $[NTf_2]$ pyridinium and imidazolium ILs was observed, the same molecular model approach previously proposed for $[NTf_2]$ imidazolium ILs has been applied to represent the cation−anion interactions. ILs belonging to the $[NTf_2]$ pyridinium family were modeled as homonuclear chainlike molecules with three associating sites. The chain length parameter, m_i, was transferred from the imidazoliums according to the number of carbons in the radicals of the cation. A set of molecular parameters for pure $[C_n\text{mpy}][NTf_2]$ and $[C_n\text{py}][NTf_2]$ ILs was fitted to liquid density data at atmospheric pressure. Furthermore, a linear trend with the molecular weight for the pyridiniums was identified for the segment diameter σ_{ii}, while the remaining three molecular parameters (ε_{ii}/k_B, K^{HB}, and $\varepsilon_{ii}^{HB}/k_B$) were kept constant for all compounds.

The surface tension of the ILs with available experimental data was also reported using the density gradient theory coupled with soft-SAFT. The surface tension description helped to discriminate the most appropriate set of parameters among some of them, providing a good atmospheric density−pressure description. A value of 418 K for ε_{ii}/k_B proved to be the most adequate and lower values for the association energy and volume than those proposed for $[NTf_2]$ imidazolium ILs were obtained, in agreement with the lower cation−anion interaction strengths of $[NTf_2]$ pyridiniums. The transferred parameters and the correlations were used to predict the molecular parameters of the compounds with longer and shorter alkyl chains in the cation. The new model was also used to predict densities at higher pressures and second-order thermodynamic derivative properties, proving the adequacy of the selected molecular model and parameter values.

Then, the CO_2 and the SO_2 solubility in $[C_n\text{mpy}][NTf_2]$ and $[C_n\text{py}][NTf_2]$ ILs was studied. A temperature-independent energy binary parameter (ξ_{ij}) was required to reach quantitative agreement with experimental data at all conditions of temperature and pressure. The values for the binary parameter were of the same order as those found for imidazolium ILs, proving the similar nature of both families. For the CO_2 case, it was possible to establish a relation between the ξ_{ij} value and the molecular weight of the IL. As done for the pure compounds, the solubility of CO_2 + $[C_{12}\text{py}][NTf_2]$ was predicted using the correlation, finding good agreement with the experimental data.

A final test of the approach and the model was performed when successfully modeling the LLE of water + $[C_n\text{mpy}][NTf_2]/[C_n\text{py}][NTf_2]$ systems. In this case, also an only binary parameter was adjusted (η_{ij}), and a trend with the molecular weight of the different ILs was identified. The calculated mutual solubilities were accurate in reproducing the experimental measurements.

The molecular models presented within the soft-SAFT framework show a high degree of accuracy and transferability to describe pure ILs thermophysical properties and the phase equilibria of their mixtures with water and gases, becoming a

dx.doi.org/10.1021/jp303166f | J. Phys. Chem. B 2012, 116, 9089−9100

valuable tool to assist the ILs design for specific industrial applications.

AUTHOR INFORMATION

Corresponding Author

*E-mail: vegal@matgas.org. Phone: +34 935 929 950. Fax: +34 935 929 951.

Notes

The authors declare no competing financial interest.

ACKNOWLEDGMENTS

The authors acknowledge the financial support from Fundação para a Ciência e a Tecnologia (FCT) for Project PTDC/EQU-FTT/102166/2008. M.B.O. acknowledges her postdoctoral grant (SFRH/BPD/71200/2010) and F.L. a TALENT contract from the Catalan Government. CICECO is being funded by FCT through Project Pest-C/CTM/LA0011/2011. Additional financial support was provided by the Spanish government, Ministerio de Economía y Competitividad (Projects CTQ2008-05370/PPQ and CENIT SOST-CO2 CEN2008-01027) and the Catalan government (Project 2009SGR-666). Support from Carburos Metálicos, Air Products Group, is also acknowledged.

REFERENCES

(1) Aparicio, S.; Atilhan, M.; Karadas, F. *Ind. Eng. Chem. Res.* **2010**, *49*, 9580−9595.
(2) Edward, W.; Castner, J.; Wishart, J. F. *J. Chem. Phys.* **2010**, *132*, No. 120901.
(3) Wilkes, J. S. *Green Chem.* **2002**, *4*, 73−80.
(4) Cadena, C.; Zhao, Q.; Snurr, R. Q.; Maginn, E. J. *J. Phys. Chem. B* **2006**, *110*, 2821−2832.
(5) Crosthwaite, J. M.; Muldoon, M. J.; Dixon, J. K.; Anderson, J. L.; Brennecke, J. F. *J. Chem. Thermodyn.* **2005**, *37*, 559−568.
(6) Gao, H.; Luo, M.; Xing, J.; Wu, Y.; Li, Y.; Li, W.; Liu, Q.; Liu, H. *Ind. Eng. Chem. Res.* **2008**, *47*, 8384−8388.
(7) Xiao, Y.; Malhotra, S. V. *Tetrahedron Lett.* **2004**, *45*, 8339−8342.
(8) Coutinho, J. A. P.; Carvalho, P.; Oliveira, M. C. *RSC Adv.* **2012**, DOI: 10.1039/C2RA20141K.
(9) Gardas, R. L.; Costa, H. F.; Freire, M. G.; Carvalho, P. J.; Marrucho, I. M.; Fonseca, I. M. A.; Ferreira, A. G. M.; Coutinho, J. A. P. *Ind. Eng. Chem. Res.* **2008**, *53*, 805−811.
(10) Gardas, R. L.; Coutinho, J. A. P. *Fluid Phase Equilib.* **2008**, *263*, 26−32.
(11) Paduszyński, K.; Domańska, U. *Ind. Eng. Chem. Res.* **2012**, *51*, 591−604.
(12) Mokhtarani, B.; Sharifi, A.; Mortaheb, H. R.; Mirzaei, M.; Mafi, M.; Sadeghian, F. *J. Chem. Thermodyn.* **2009**, *41*, 323−329.
(13) Sánchez, L. G.; Espel, J. R.; Onink, F.; Meindersma, G. W.; Haan, A. B. D. *J. Chem. Eng. Data* **2009**, *54*, 2803−2812.
(14) Bandrés, I.; Giner, B.; Artigas, H.; Lafuente, C.; Royo, F. M. *J. Chem. Eng. Data* **2009**, *54*, 236−240.
(15) Dutt, N. V. K.; Ravikumar, Y. V. L. 3rd National Conference on Thermodynamics of Chemical and Biological Systems, Nagpur, India, 2008.
(16) Gardas, R. L.; Coutinho, J. A. P. *AIChE J.* **2009**, *55*, 1274−1290.
(17) Paduszyński, K.; Domańska, U. *J. Phys. Chem. B* **2012**, *116*, 5002−5018.
(18) Dreiseitlová, J.; Rehák, K.; Vreekamp, R. *J. Chem. Eng. Data* **2010**, *55*, 3051−3054.
(19) Crosthwaite, J. M.; Muldoon, M. J.; Aki, S. N. V. K.; Maginn, E. J.; Brennecke, J. F. *J. Phys. Chem. B* **2006**, *110*, 9354−9361.
(20) Chapeaux, A.; Simoni, L. D.; Stadtherr, M. A.; Brennecke, J. F. *J. Chem. Eng. Data* **2007**, *52*, 2462−2467.
(21) García, J.; García, S.; Torrecilla, J. S.; Rodríguez, F. *Fluid Phase Equilib.* **2011**, *301*, 62−66.
(22) Domańska, U.; Królikowski, M.; Ramjugernath, D.; Letcher, T. M.; Tumba, K. *J. Phys. Chem. B* **2010**, *114*, 15011−15017.
(23) Lazzús, J.; Marín, J. *J. Eng. Thermophys.* **2010**, *19*, 170−183.
(24) Hosseini, S. *Ionics* **2010**, *16*, 571−575.
(25) Martín, A.; Méndez, D.; Bermejo, M. D. *J. Chem. Thermodyn.* **2010**, *42*, 524−529.
(26) Bermejo, M. D.; Méndez, D.; Martín, A. *Ind. Eng. Chem. Res.* **2010**, *49*, 4966−4973.
(27) Freire, M. G.; Neves, C. M. S. S.; Carvalho, P. J.; Gardas, R. L.; Fernandes, A. M.; Marrucho, I. M.; Santos, L. M. N. B. F.; Coutinho, J. A. P. *J. Phys. Chem. B* **2007**, *111*, 13082−13089.
(28) Freire, M. G.; Santos, L. M. N. B. F.; Marrucho, I. M.; Coutinho, J. A. *Fluid Phase Equilib.* **2007**, *255*, 167−178.
(29) Ferreira, A. R.; Freire, M. G.; Ribeiro, J. C.; Lopes, F. M.; Crespo, J. G.; Coutinho, J. A. P. *Ind. Eng. Chem. Res.* **2011**, *50*, 5279−5294.
(30) Ferreira, A. R.; Freire, M. G.; Ribeiro, J. C.; Lopes, F. M.; Crespo, J. G.; Coutinho, J. A. P. *Ind. Eng. Chem. Res.* **2012**, *51*, 3483−3507.
(31) Sistla, Y. S.; Khanna, A. *J. Chem. Eng. Data* **2011**, *56*, 4045−4060.
(32) Chapman, W. G.; Gubbins, K. E.; Jackson, G.; Radosz, M. *Fluid Phase Equilib.* **1989**, *52*, 31−38.
(33) Huang, S. H.; Radosz, M. *Ind. Eng. Chem. Res.* **1990**, *29*, 2284−2294.
(34) Blas, F. J.; Vega, L. F. *Mol. Phys.* **1997**, *92*, 135−150.
(35) Andreu, J. S.; Vega, L. F. *J. Phys. Chem. C* **2007**, *111*, 16028−16034.
(36) Andreu, J. S.; Vega, L. F. *J. Phys. Chem. B* **2008**, *112*, 15398−15406.
(37) Llovell, F.; Valente, E.; Vilaseca, O.; Vega, L. F. *J. Phys. Chem. B* **2011**, *115*, 4387−4398.
(38) Llovell, F.; Vilaseca, O.; Vega, L. F. *Sep. Sci. Technol.* **2012**, *47*, 399−410.
(39) Vega, L. F.; Vilaseca, O.; Llovell, F.; Andreu, J. S. *Fluid Phase Equilib.* **2010**, *294*, 15−30.
(40) Llovell, F.; Marcos, R. M.; MacDowell, N.; Vega, L. F. *J. Phys. Chem. B* **2012**, in press.
(41) Wertheim, M. S. *J. Stat. Phys.* **1984**, *35*, 35−47.
(42) Wertheim, M. S. *J. Stat. Phys.* **1986**, *42*, 477−492.
(43) Müller, E. A.; Gubbins, K. E. *Ind. Eng. Chem. Res.* **2001**, *40*, 2193−2211.
(44) Economou, I. G. *Ind. Eng. Chem. Res.* **2002**, *41*, 953−962.
(45) Johnson, J. K.; Zollweg, J. A.; Gubbins, K. E. *Mol. Phys.* **1993**, *78*, 591−618.
(46) Johnson, J. K.; Mueller, E. A.; Gubbins, K. E. *J. Phys. Chem. B* **1994**, *98*, 6413−6419.
(47) Gubbins, K. E.; Twu, C. H. *Chem. Eng. Sci.* **1978**, *33*, 863−878.
(48) Jog, P. K.; Sauer, S. G.; Blaesing, J.; Chapman, W. G. *Ind. Eng. Chem. Res.* **2001**, *40*, 4641−4648.
(49) Stell, G.; Rasaiah, J.; Narang, H. *Mol. Phys.* **1974**, *27*, 1393−1414.
(50) van der Waals, J. D. *J. Stat. Phys.* **1979**, *20*, 200−244.
(51) Cahn, J. W.; Hilliard, J. E. *J. Chem. Phys.* **1958**, *28*, 258−267.
(52) Bongiorno, V.; Scriven, L.; Davis, H. *J. Colloid Interface Sci.* **1976**, *57*, 462−475.
(53) Vilaseca, O.; Vega, L. F. *Fluid Phase Equilib.* **2011**, *306*, 4−14.
(54) van der Waals, J. D. *Z. Phys. Chem. Leipzig* **1894**, *13*, 657−725.
(55) Duque, D.; Pàmies, J. C.; Vega, L. F. *J. Chem. Phys.* **2004**, *121*, 11395−11401.
(56) Marcus, Y.; Hefter, G. *Chem. Rev.* **2006**, *106*, 4585−4621.
(57) Yokozeki, A.; Kasprzak, D. J.; Shiflett, M. B. *Phys. Chem. Chem. Phys.* **2007**, *9*, 5018−5026.
(58) Weingartner, H. *Angew. Chem., Int. Ed.* **2008**, *47*, 654−670.
(59) Weiss, V. C.; Heggen, B.; Müller-Plathe, F. *J. Phys. Chem. C* **2010**, *114*, 3599−3608.
(60) Freire, M. G.; Neves, C. M. S. S.; Shimizu, K.; Bernardes, C. E. S.; Marrucho, I. M.; Coutinho, J. A. P.; Lopes, J. N. C.; Rebelo, L. P. N. *J. Phys. Chem. B* **2010**, *114*, 15925−15934.

(61) Vega, L. F.; Llovell, F.; Blas, F. J. *J. Phys. Chem. B* **2009**, *113*, 7621−7630.
(62) Dias, A. M. A.; Carrier, H.; Daridon, J. L.; Pàmies, J. C.; Vega, L. F.; Coutinho, J. A. P.; Marrucho, I. M. *Ind. Eng. Chem. Res.* **2006**, *45*, 2341−2350.
(63) Battaglia, M. R.; Buckingham, A. D.; Neumark, D.; Pierens, R. K.; Williams, J. H. *Mol. Phys.* **1981**, *43*, 1015−1020.
(64) Graham, C.; Pierrus, J.; Raab, R. E. *Mol. Phys.* **1989**, *67*, 939−955.
(65) Llovell, F.; Florusse, L. J.; Peters, C. J.; Vega, L. F. *J. Phys. Chem. B* **2007**, *111*, 10180−10188.
(66) Deng, Y.; Husson, P.; Delort, A.; Besse-Hoggan, P.; Sancelme, M.; Costa Gomes, M. F. *J. Chem. Eng. Data* **2011**, *56*, 4194−4202.
(67) Liu, Q.; Yang, M.; Yan, P.; Liu, X.; Tan, Z.; Welz-Biermann, U. *J. Chem. Eng. Data* **2010**, *55*, 4928−4930.
(68) Oliveira, F. S.; Freire, M. G.; Carvalho, P. J.; Coutinho, J. A. P.; Lopes, J. N. C.; Rebelo, L. P. N.; Marrucho, I. M. *J. Chem. Eng. Data* **2010**, *55*, 4514−4520.
(69) Tokuda, H.; Ishii, K.; Susan, M. A. B. H.; Tsuzuki, S.; Hayamizu, K.; Watanabe, M. *J. Phys. Chem. B* **2006**, *110*, 2833−2839.
(70) Yunus, N. M.; Mutalib, M. A.; Man, Z.; Bustam, M. A.; Murugesan, T. *J. Chem. Thermodyn.* **2010**, *42*, 491−495.
(71) Kato, R.; Gmehling, J. *Fluid Phase Equilib.* **2004**, *226*, 37−44.
(72) Liu, Q.; Yang, M.; Li, P.; Sun, S.; Welz-Biermann, U.; Tan, Z.; Zhang, Q. *J. Chem. Eng. Data* **2011**, *56*, 4094−4101.
(73) Fernandes, A. M.; Rocha, M. A. A.; Freire, M. G.; Marrucho, I. M.; Coutinho, J. A. P.; Santos, L. M. N. B. F. *J. Phys. Chem. B* **2011**, *115*, 4033−4041.
(74) Carvalho, P. J.; Neves, C. M. S. S.; Coutinho, J. A. P. *J. Chem. Eng. Data* **2010**, *55*, 3807−3812.
(75) Ohlin, C. A.; Dyson, P. J.; Laurenczy, G. *Chem. Commun. (Cambridge, UK)* **2004**, 1070−1071.
(76) Seoane, R. G.; Corderí, S.; Gomez, E.; Calvar, N.; González, E. J.; Macedo, E.; Domínguez, A. *Ind. Eng. Chem. Res.* **2012**, *51*, 2492−2504.
(77) Gardas, R. L.; Costa, H. F.; Freire, M. G.; Carvalho, P. J.; Marrucho, I. M.; Fonseca, I. M. A.; Ferreira, A. G. M.; Coutinho, J. A. P. *J. Chem. Eng. Data* **2008**, *53*, 805−811.
(78) Carvalho, P. J.; Álvarez, V. H.; Marrucho, I. M.; Aznar, M.; Coutinho, J. A. *J. Supercrit. Fluids* **2009**, *50*, 105−111.
(79) Yunus, N. M.; Mutalib, M. A.; Man, Z.; Bustam, M. A.; Murugesan, T. *Chem. Eng. J.* **2012**, *189−190*, 94−100.
(80) Hou, Y.; Baltus, R. E. *Ind. Eng. Chem. Res.* **2007**, *46*, 8166−8175.
(81) Muldoon, M. J.; Aki, S. N. V. K.; Anderson, J. L.; Dixon, J. K.; Brennecke, J. F. *J. Phys. Chem. B* **2007**, *111*, 9001−9009.
(82) Anderson, J. L.; Dixon, J. K.; Maginn, E. J.; Brennecke, J. F. *J. Phys. Chem. B* **2006**, *110*, 15059−15062.
(83) Blas, F. J.; Vega, L. F. *Ind. Eng. Chem. Res.* **1998**, *37*, 660−674.
(84) Pàmies, J. C.; Vega, L. F. *Ind. Eng. Chem. Res.* **2001**, *40*, 2532−2543.
(85) Freire, M. G.; Santos, L. M. N. B. F.; Fernandes, A. M.; Coutinho, J. A. P.; Marrucho, I. M. *Fluid Phase Equilib.* **2007**, *261*, 449−454.